Mark Blonquist
Bruce Bugbee

Sensor Update
October 13 & 16, 2006

Overview

- **Infra-red Sensor**
  - Advantages
  - Calibration
  - Applications
- **Pyranometers**
  - Cosine Response
  - Long-term Drift

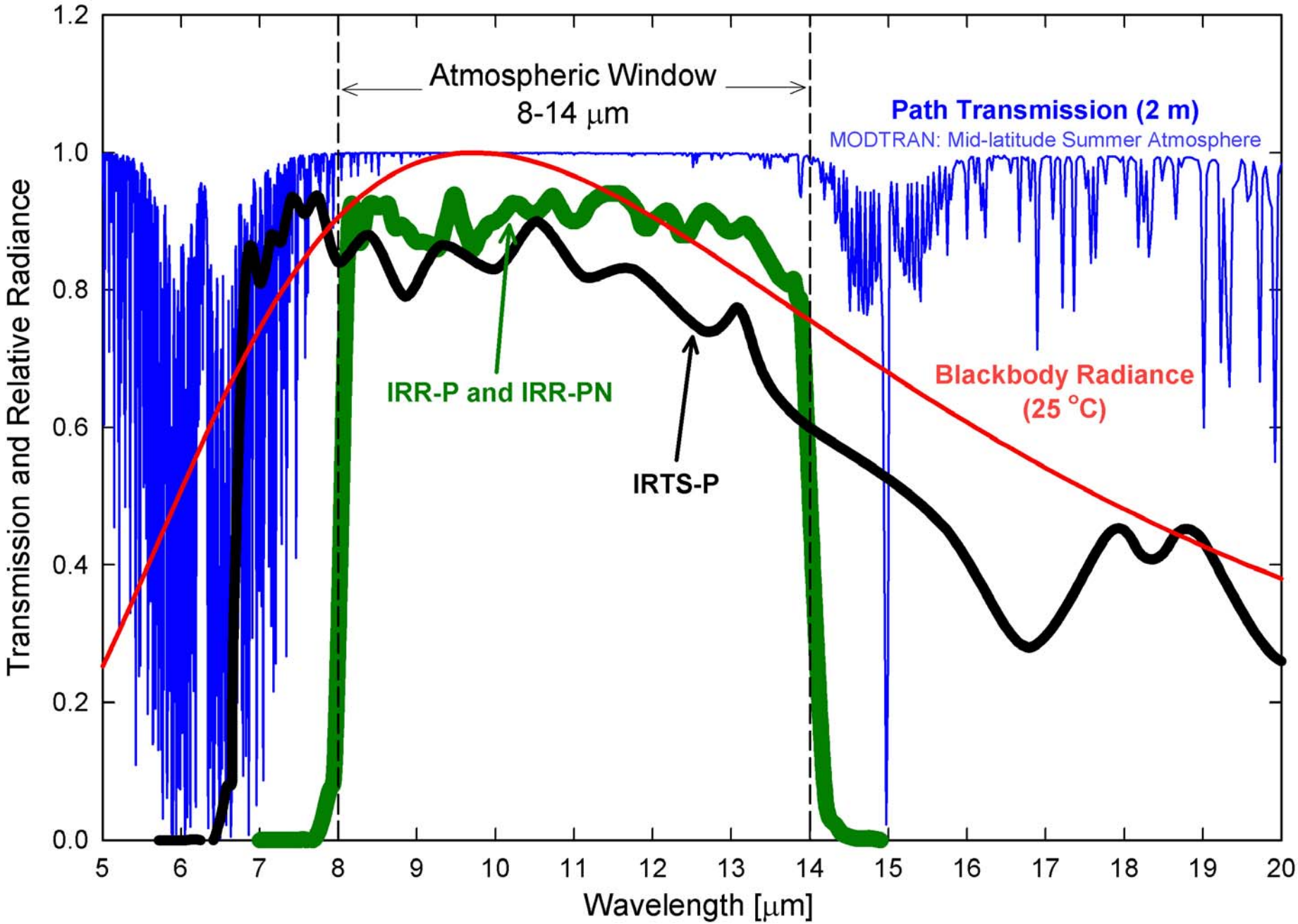
Atmospheric Window
8-14 μm
Path Transmission (2 m)
MODTRAN: Mid-latitude Summer Atmosphere
IRR-P and IRR-PN
IRTS-P
Blackbody Radiance
(25 °C)
Transmission and Relative Radiance
Wavelength [μm]
1.2
1.0
0.8
0.6
0.4
0.2
0.0
5
6
7
8
9
10
11
12
13
14
15
16
17
18
19
20

Field of view (FOV)
IRR-P half-angle = 22˚
IRR-PN half-angle = 18˚
IRTS-P half-angle = 28˚

The FOV is reported as the half-angle of the apex of the cone formed by the target (cone base) and the detector (cone apex). The target is a circle from which 98% of the radiation viewed by the detector is being emitted.

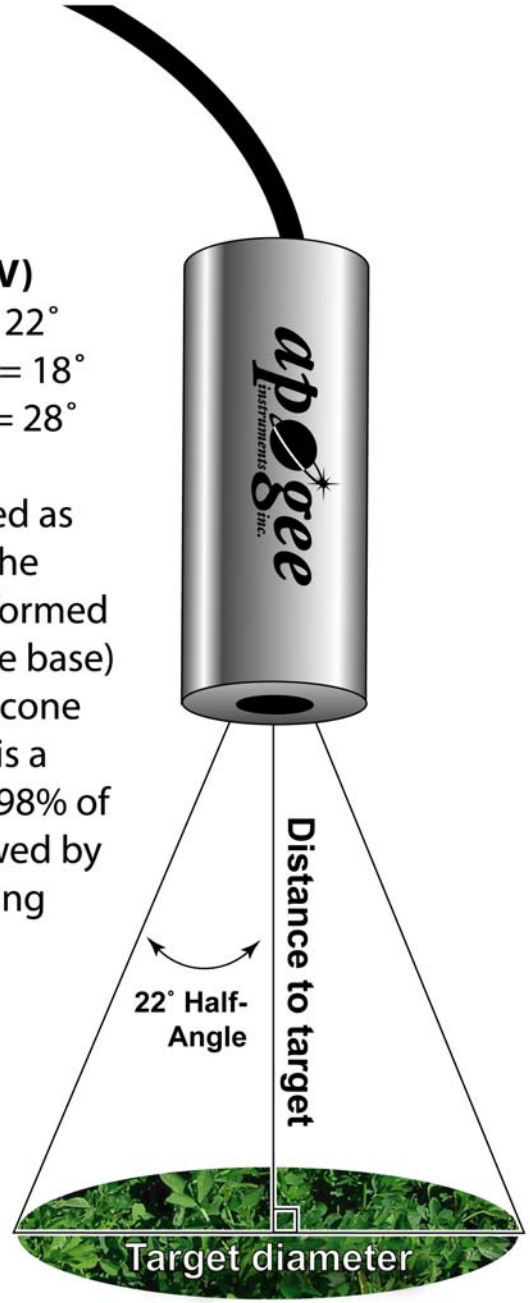

FOV Determination with Leslie Cube

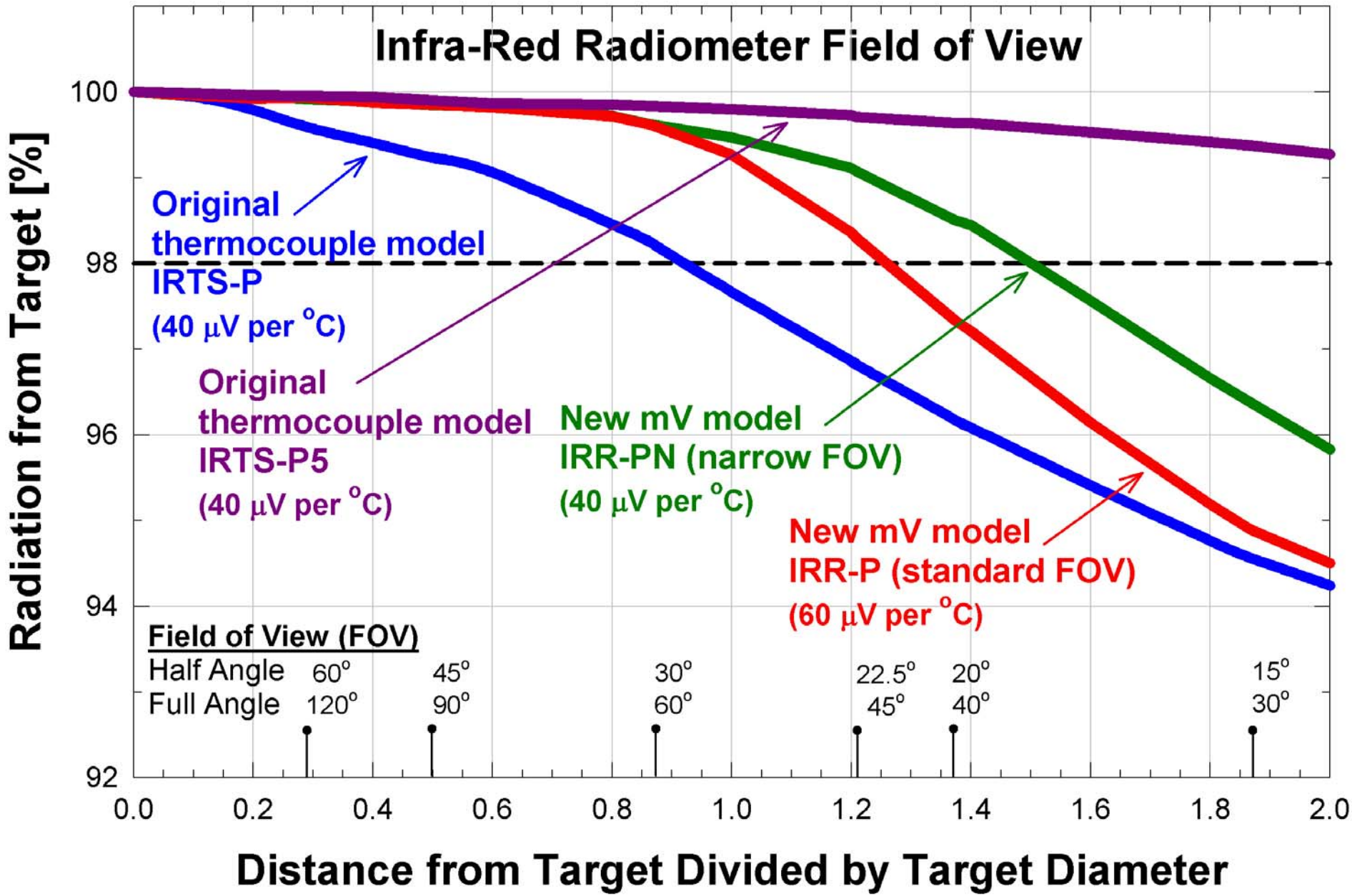
Infra-Red Radiometer Field of View
Radiation from Target [%]
100
98
96
94
92
0.0
0.2
0.4
0.6
0.8
1.0
1.2
1.4
1.6
1.8
2.0
Distance from Target Divided by Target Diameter
Original thermocouple model IRTS-P (40 μV per °C)
Original thermocouple model IRTS-P5 (40 μV per °C)
New mV model IRR-PN (narrow FOV) (40 μV per °C)
New mV model IRR-P (standard FOV) (60 μV per °C)
Field of View (FOV)
Half Angle 60° 45° 30° 22.5° 20° 15°
Full Angle 120° 90° 60° 45° 40° 30°


apogee
instruments inc.
apogee
instruments inc.

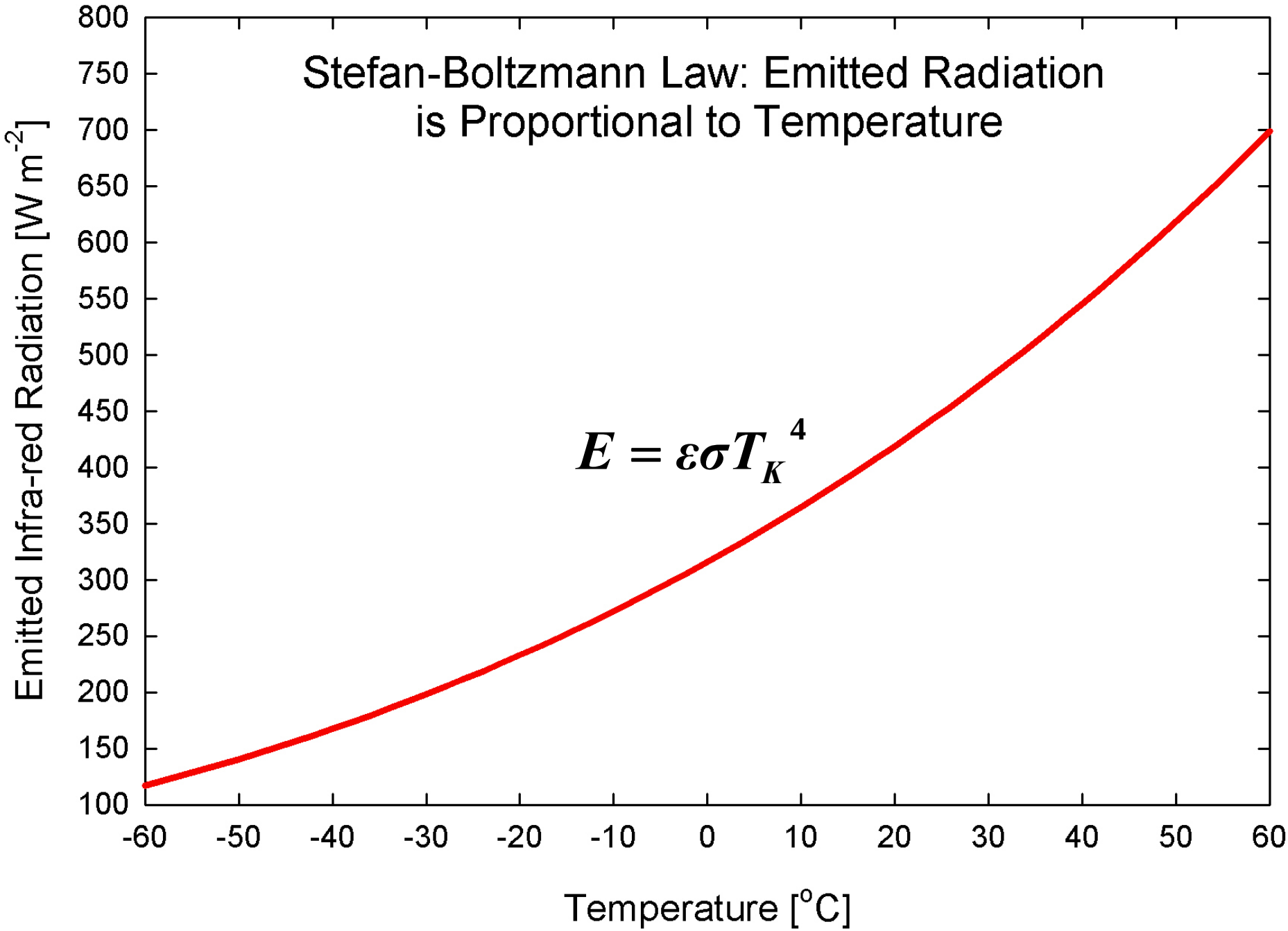
Stefan-Boltzmann Law: Emitted Radiation
is Proportional to Temperature
$E = \varepsilon\sigma T_K^4$
Emitted Infra-red Radiation [W m^{-2}]
800
750
700
650
600
550
500
450
400
350
300
250
200
150
100
-60
-50
-40
-30
-20
-10
0
10
20
30
40
50
60
Temperature [°C]

Calibration Equation

- Kalma et al. (Calibration of small infra-red surface temperature transducers, Ag. For. Met, 1988) proposed:

$$T_T^{\,4} - T_D^{\,4} = m \cdot mV + b$$

$$T_T = \left(T_D^{\,4} + m \cdot mV + b\right)^{\frac{1}{4}}$$

- IRR-Ps were tested and found to follow the same relationship; 2nd order polynomial correction was replaced

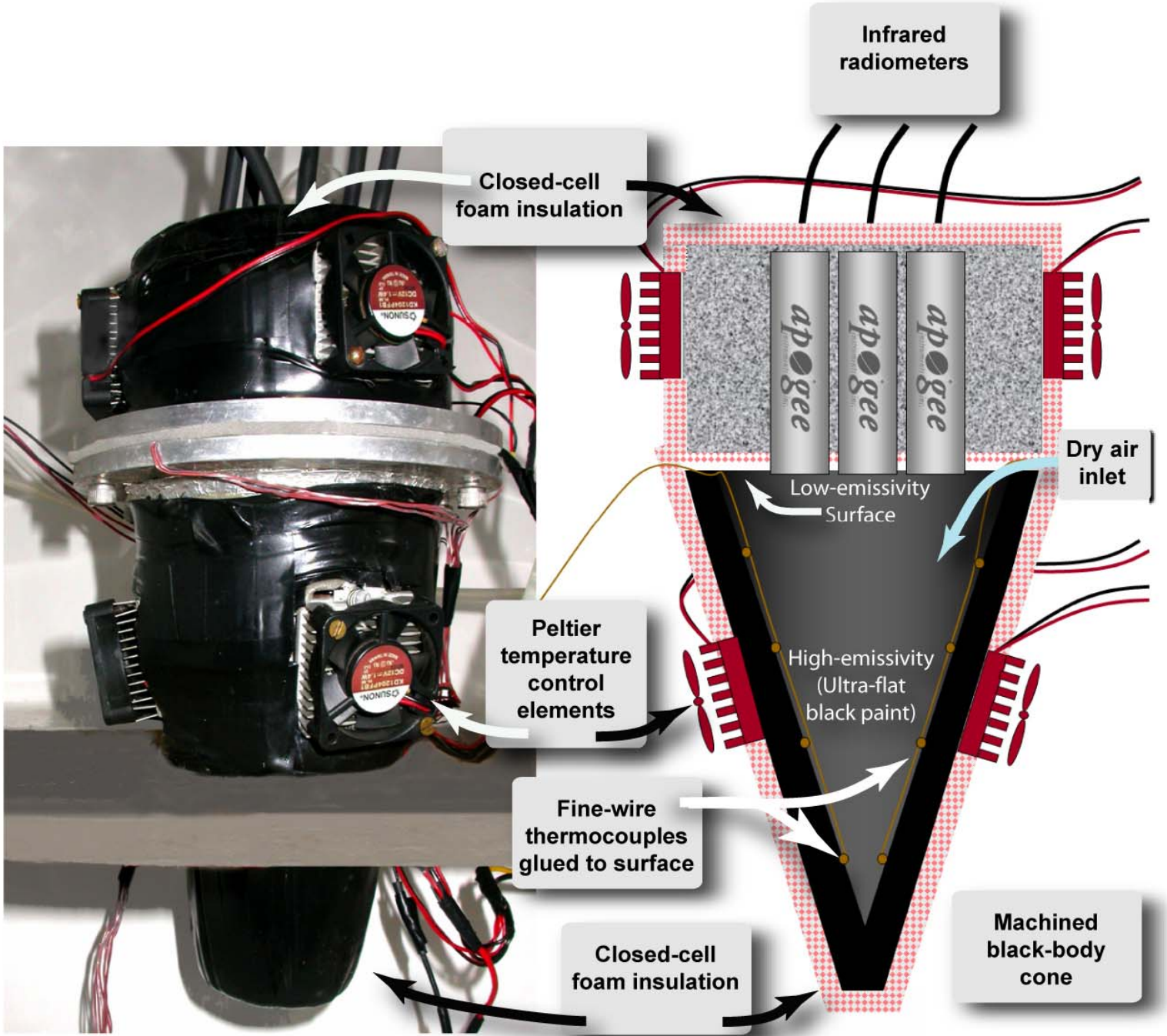
Infrared radiometers
Closed-cell foam insulation
apogee
apogee
apogee
Dry air inlet
Low-emissivity Surface
Peltier temperature control elements
High-emissivity (Ultra-flat black paint)
Fine-wire thermocouples glued to surface
Closed-cell foam insulation
Machined black-body cone

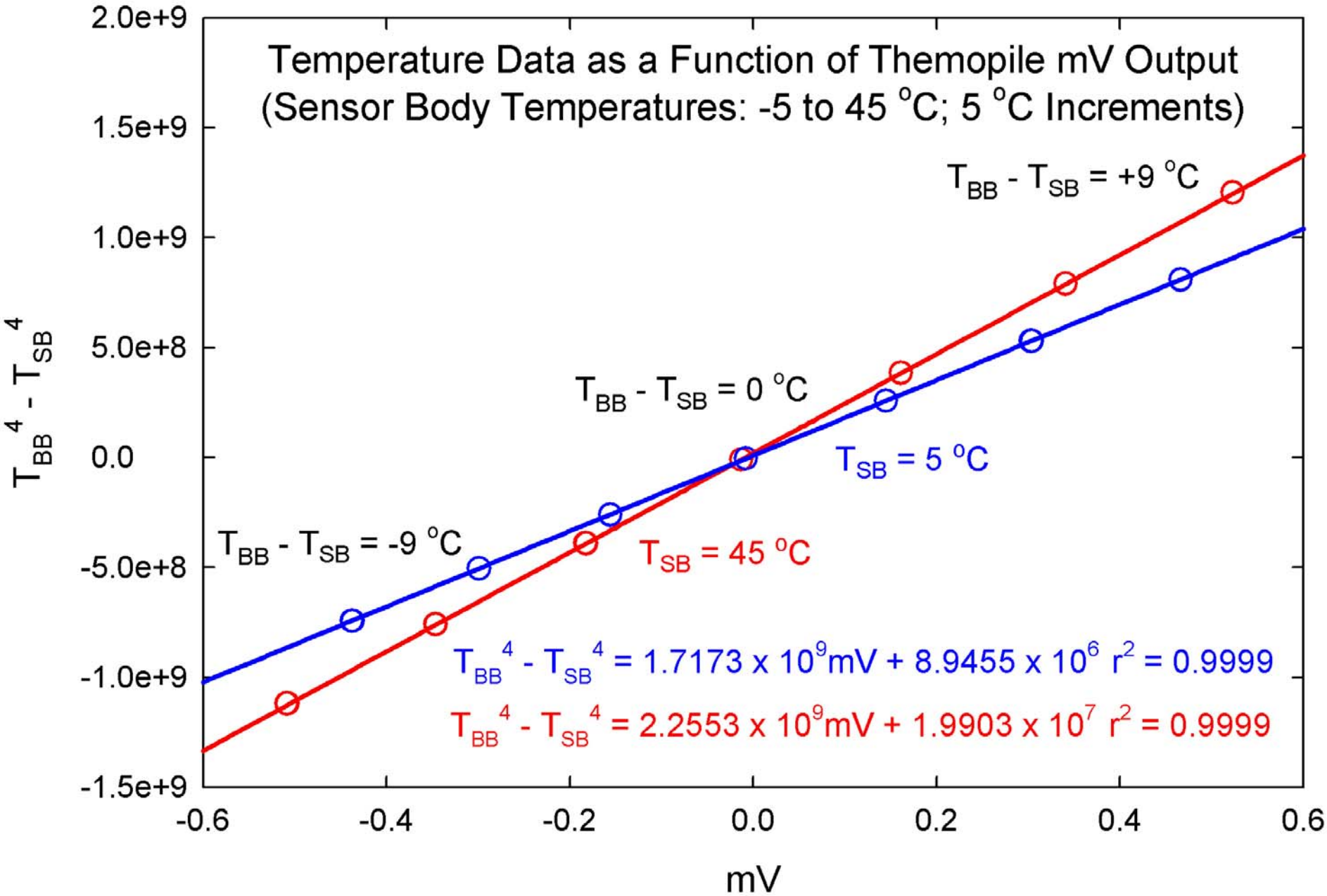
Temperature Data as a Function of Themopile mV Output
(Sensor Body Temperatures: -5 to 45 °C; 5 °C Increments)
T_{BB} - T_{SB} = +9 °C
T_{BB} - T_{SB} = 0 °C
T_{BB} - T_{SB} = -9 °C
T_{SB} = 5 °C
T_{SB} = 45 °C
T_{BB}^4 - T_{SB}^4 = 1.7173 x 10^9mV + 8.9455 x 10^6 r^2 = 0.9999
T_{BB}^4 - T_{SB}^4 = 2.2553 x 10^9mV + 1.9903 x 10^7 r^2 = 0.9999
T_{BB}^4 - T_{SB}^4
2.0e+9
1.5e+9
1.0e+9
5.0e+8
0.0
-5.0e+8
-1.0e+9
-1.5e+9
-0.6
-0.4
-0.2
0.0
0.2
0.4
0.6
mV

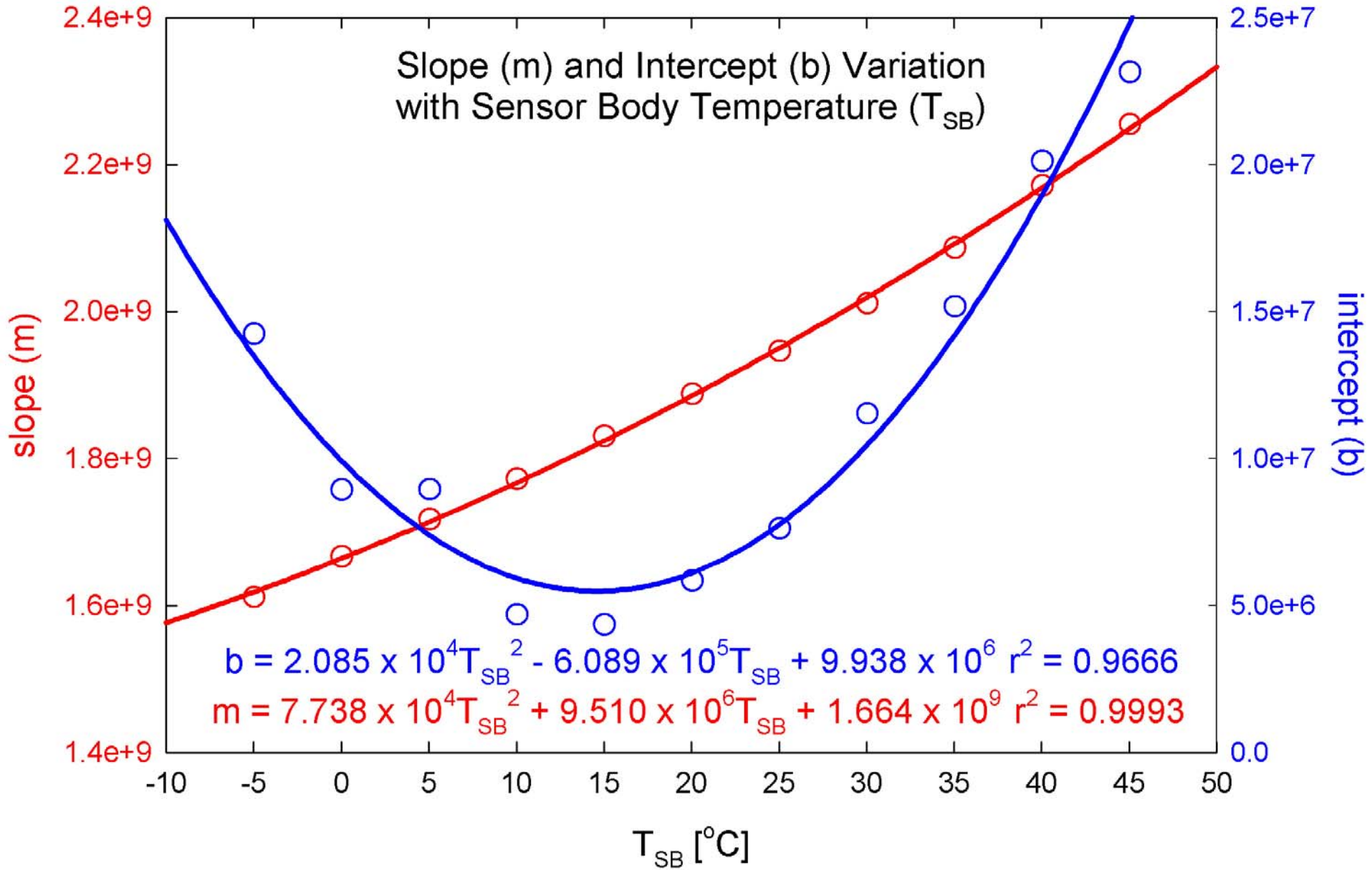
Slope (m) and Intercept (b) Variation
with Sensor Body Temperature (T_{SB})
slope (m)
intercept (b)
2.4e+9
2.2e+9
2.0e+9
1.8e+9
1.6e+9
1.4e+9
2.5e+7
2.0e+7
1.5e+7
1.0e+7
5.0e+6
0.0
-10
-5
0
5
10
15
20
25
30
35
40
45
50
T_{SB} [°C]
$b = 2.085 \times 10^4 T_{SB}^2 - 6.089 \times 10^5 T_{SB} + 9.938 \times 10^6$ $r^2 = 0.9666$
$m = 7.738 \times 10^4 T_{SB}^2 + 9.510 \times 10^6 T_{SB} + 1.664 \times 10^9$ $r^2 = 0.9993$

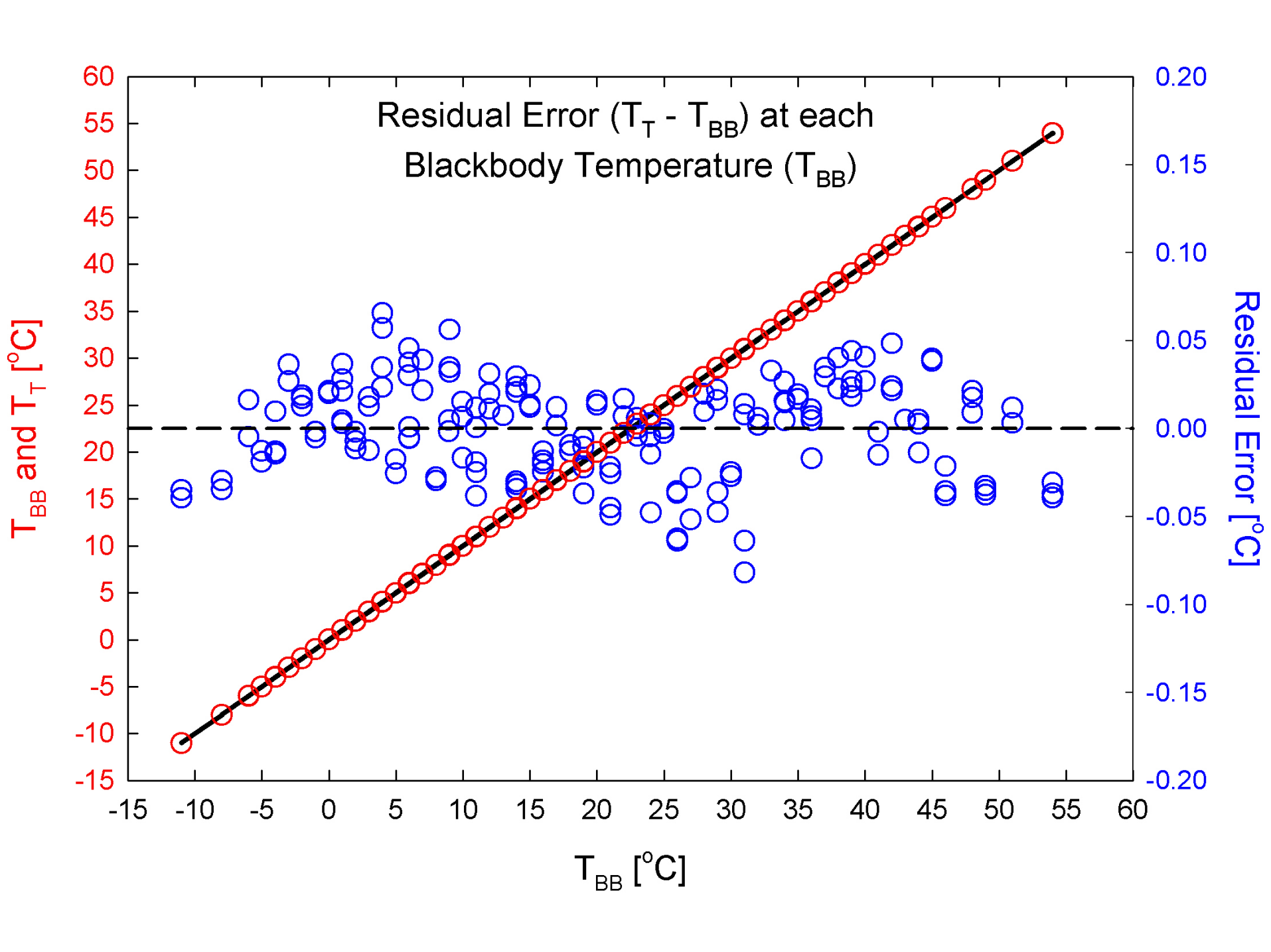
Residual Error (T_T - T_{BB}) at each
Blackbody Temperature (T_{BB})
T_{BB} and T_T [°C]
Residual Error [°C]
T_{BB} [°C]
60
55
50
45
40
35
30
25
20
15
10
5
0
-5
-10
-15
0.20
0.15
0.10
0.05
0.00
-0.05
-0.10
-0.15
-0.20
-15
-10
-5
0
5
10
15
20
25
30
35
40
45
50
55
60

Infra-red Temperature Applications

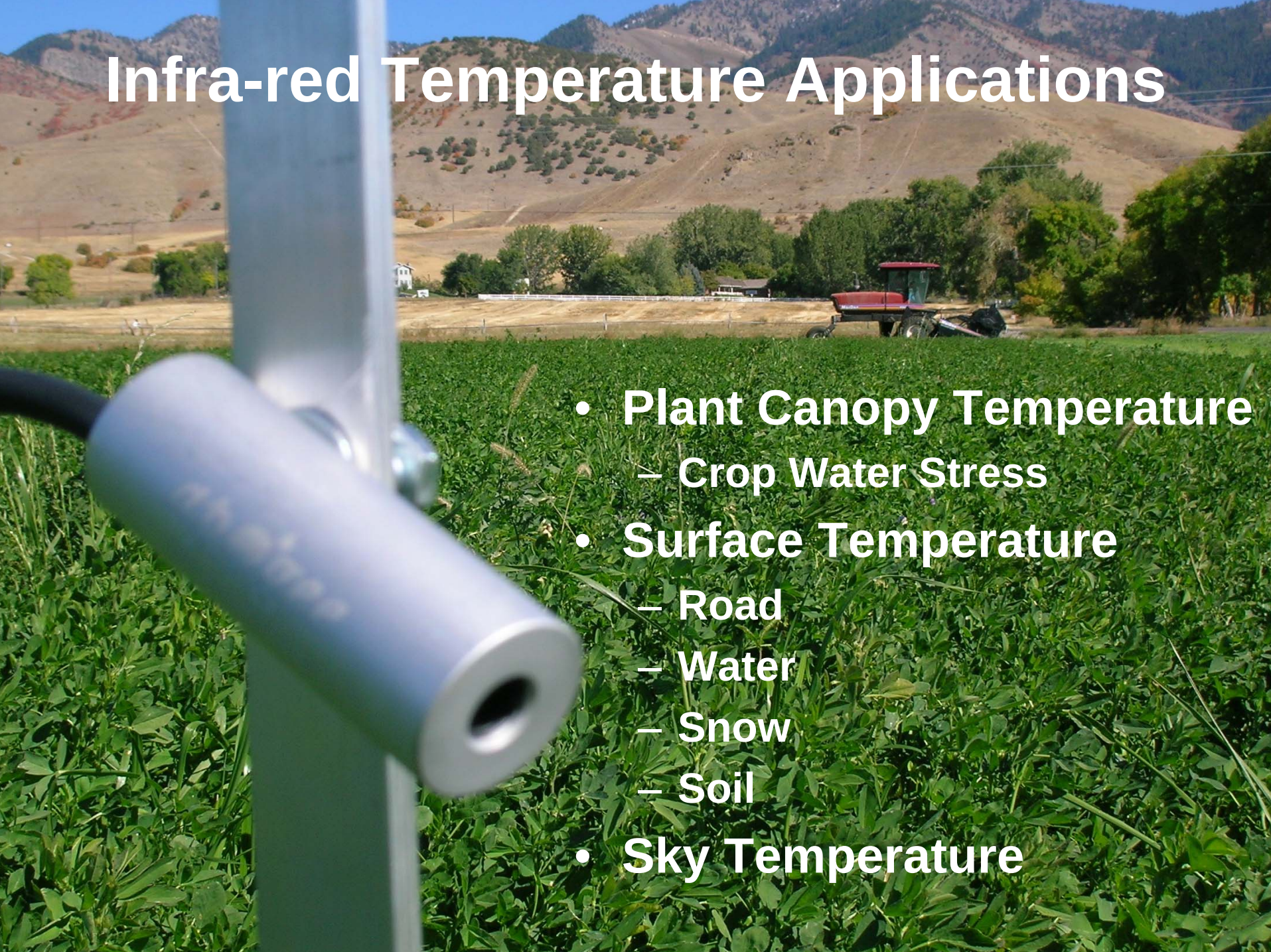

- **Plant Canopy Temperature**
  - Crop Water Stress
- **Surface Temperature**
  - Road
  - Water
  - Snow
  - Soil
- **Sky Temperature**

Crop Water Stress Index (CWSI)

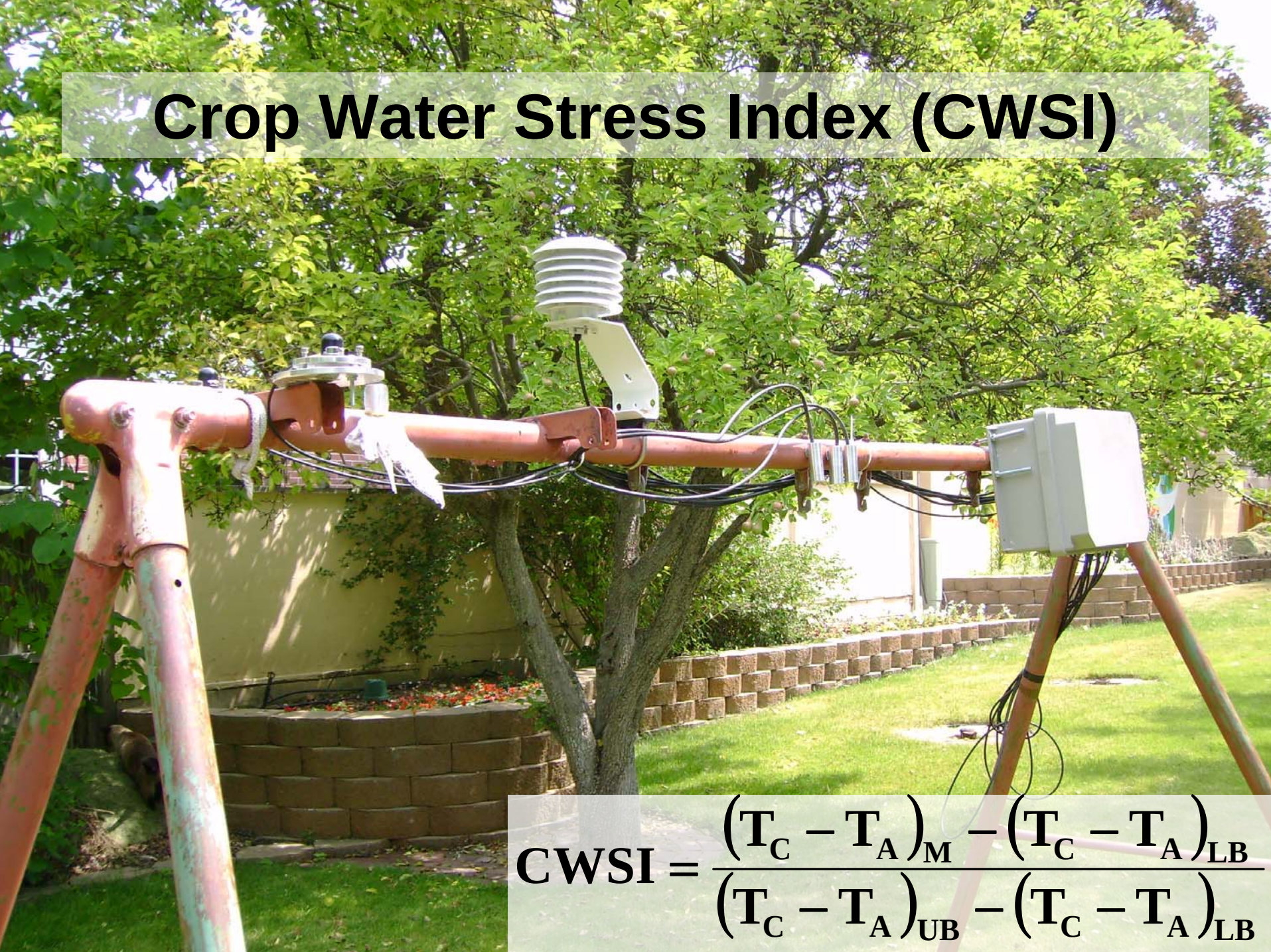

$$CWSI = \frac{(T_C - T_A)_M - (T_C - T_A)_{LB}}{(T_C - T_A)_{UB} - (T_C - T_A)_{LB}}$$

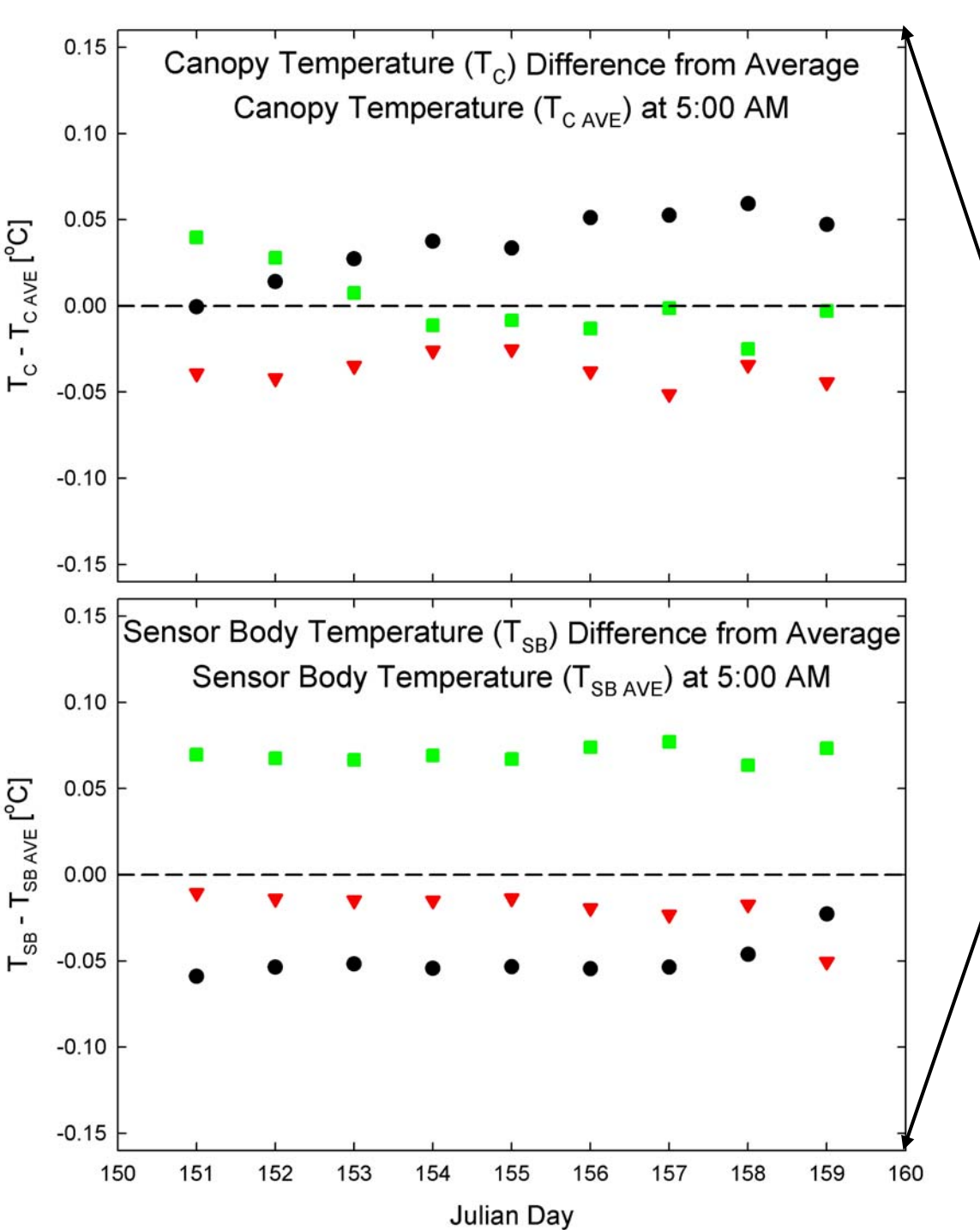
Canopy Temperature (T_C) Difference from Average
Canopy Temperature ($T_{C\ AVE}$) at 5:00 AM
$T_C - T_{C\ AVE}$ [°C]
Sensor Body Temperature (T_{SB}) Difference from Average
Sensor Body Temperature ($T_{SB\ AVE}$) at 5:00 AM
$T_{SB} - T_{SB\ AVE}$ [°C]
0.15
0.10
0.05
0.00
-0.05
-0.10
-0.15
150
151
152
153
154
155
156
157
158
159
160
Julian Day

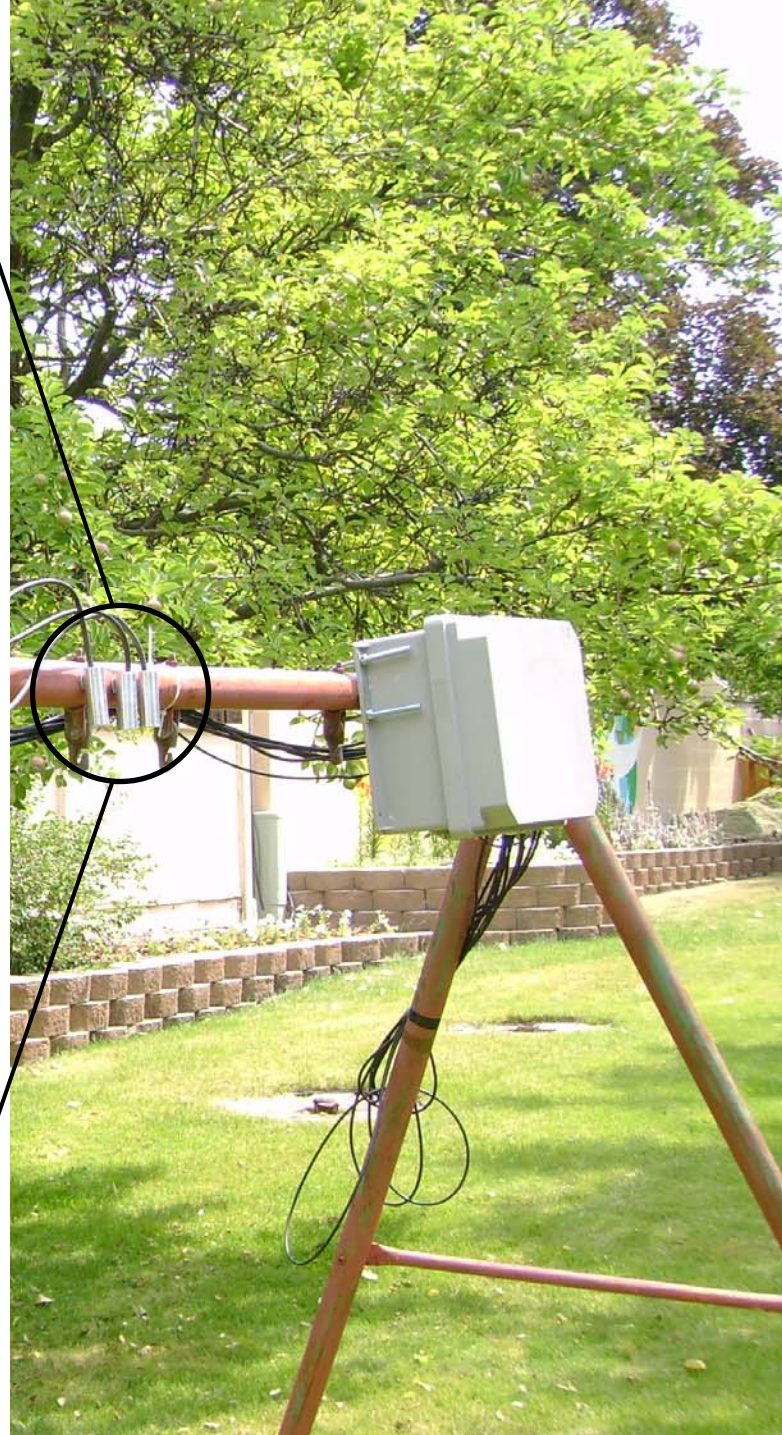

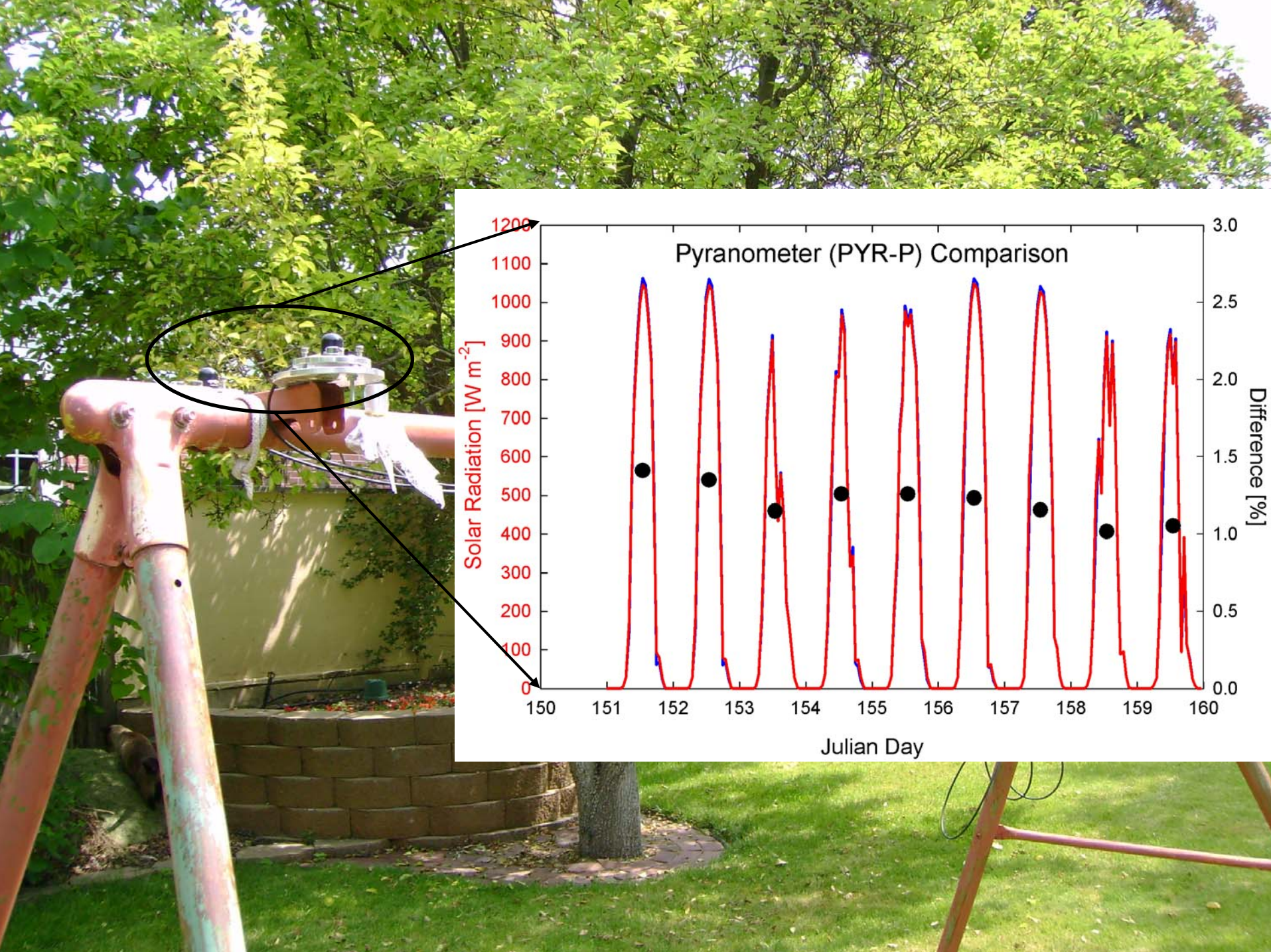
Pyranometer (PYR-P) Comparison
Solar Radiation [W m-2]
Difference [%]
Julian Day
0
100
200
300
400
500
600
700
800
900
1000
1100
1200
0.0
0.5
1.0
1.5
2.0
2.5
3.0
150
151
152
153
154
155
156
157
158
159
160

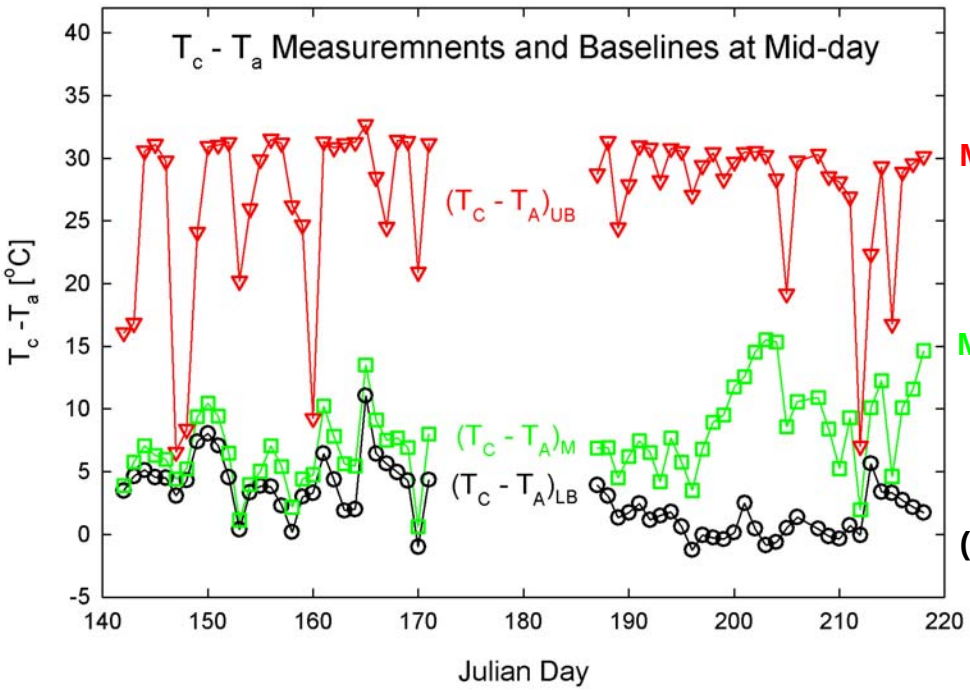
T_c - T_a Measuremnents and Baselines at Mid-day
T_c -T_a [°C]
Julian Day
$(T_C - T_A)_{UB}$
$(T_C - T_A)_M$
$(T_C - T_A)_{LB}$
Maximum stress (calculated)
Measured stress
No stress (calculated)

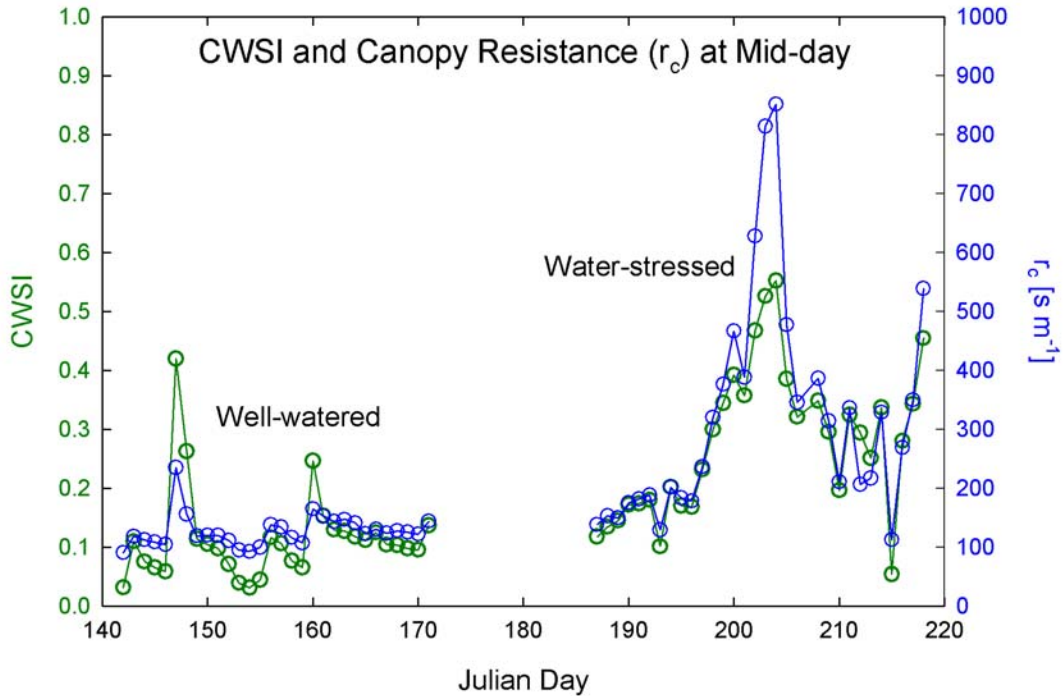
CWSI and Canopy Resistance (r_c) at Mid-day
CWSI
r_c [s m^{-1}]
Julian Day
Well-watered
Water-stressed

USU Long-Term Pyranometer Study:

Cosine Response and Daily Total Radiation Measurements

Silicon-cells:

- 3 Kipp & Zonen SP-Lites
- 4 LI-COR LI200Xs
- 6 Apogee PYR-Ps

Thermopiles:

- 3 Kipp & Zonen CM3s
- 2 Kipp & Zonen CMP3s
- 2 Hukseflux LP02s
- 3 Eppley PSPs

Reference:

- 1 Kipp & Zonen CM21 (heated and ventilated)

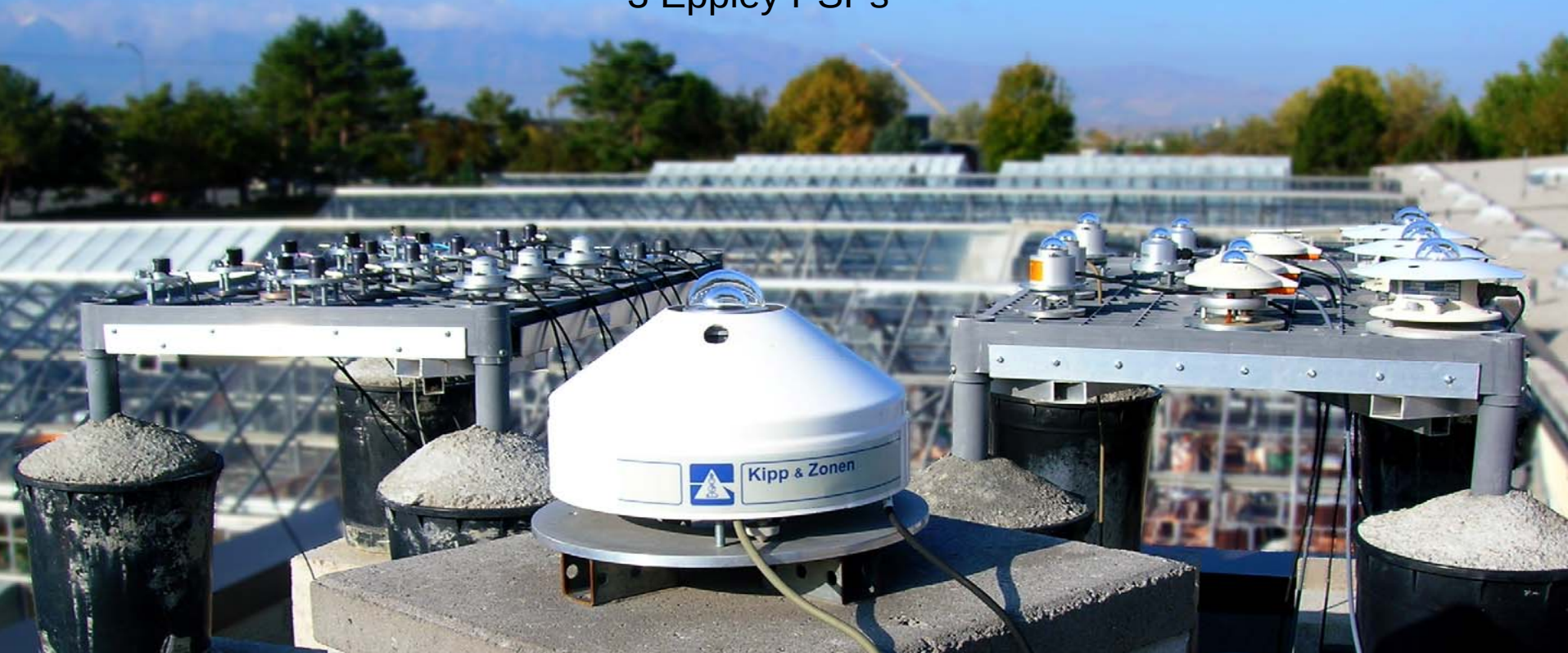

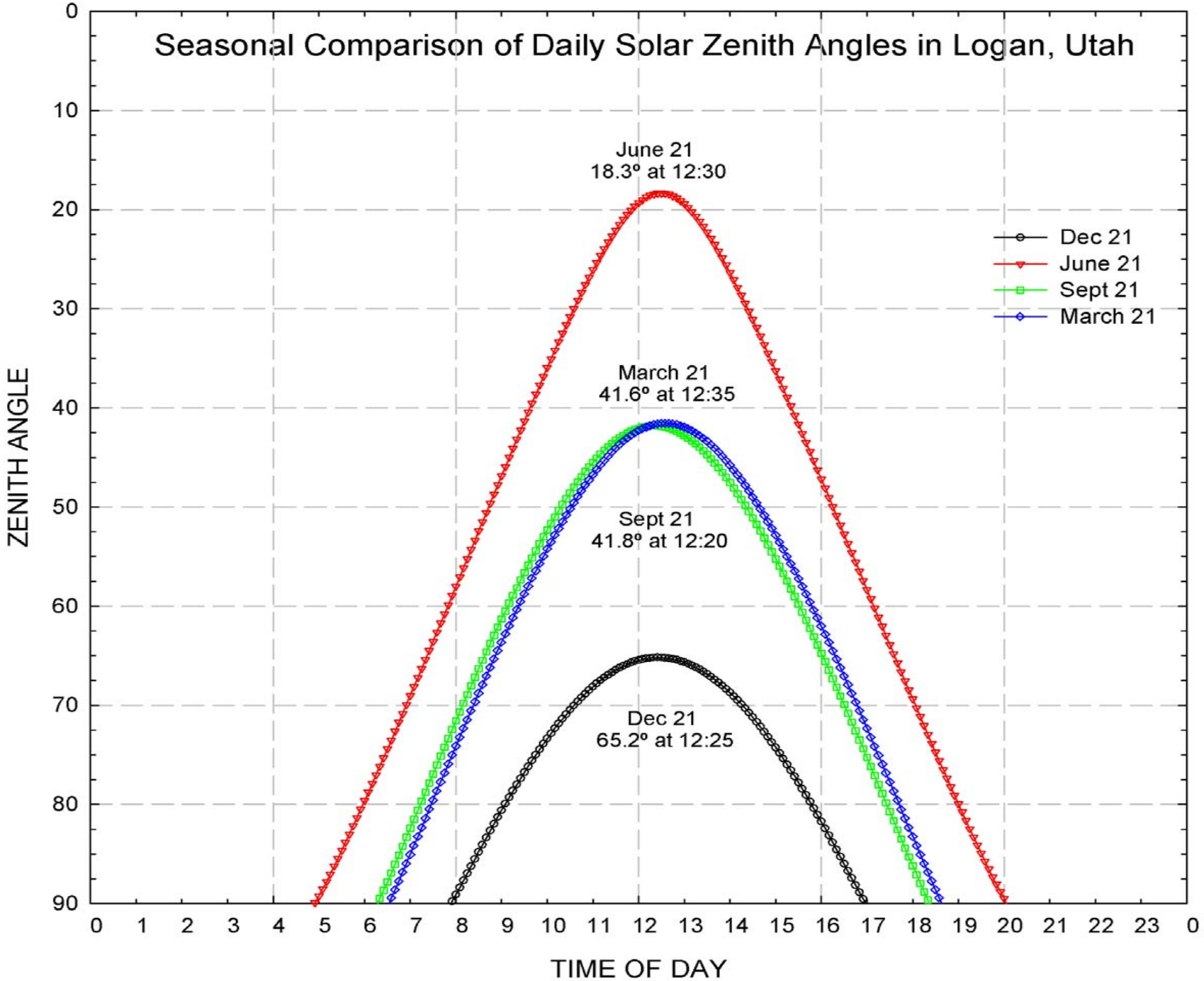
Seasonal Comparison of Daily Solar Zenith Angles in Logan, Utah
June 21
18.3º at 12:30
March 21
41.6º at 12:35
Sept 21
41.8º at 12:20
Dec 21
65.2º at 12:25
Dec 21
June 21
Sept 21
March 21
ZENITH ANGLE
TIME OF DAY
0
10
20
30
40
50
60
70
80
90
0 1 2 3 4 5 6 7 8 9 10 11 12 13 14 15 16 17 18 19 20 21 22 23 0

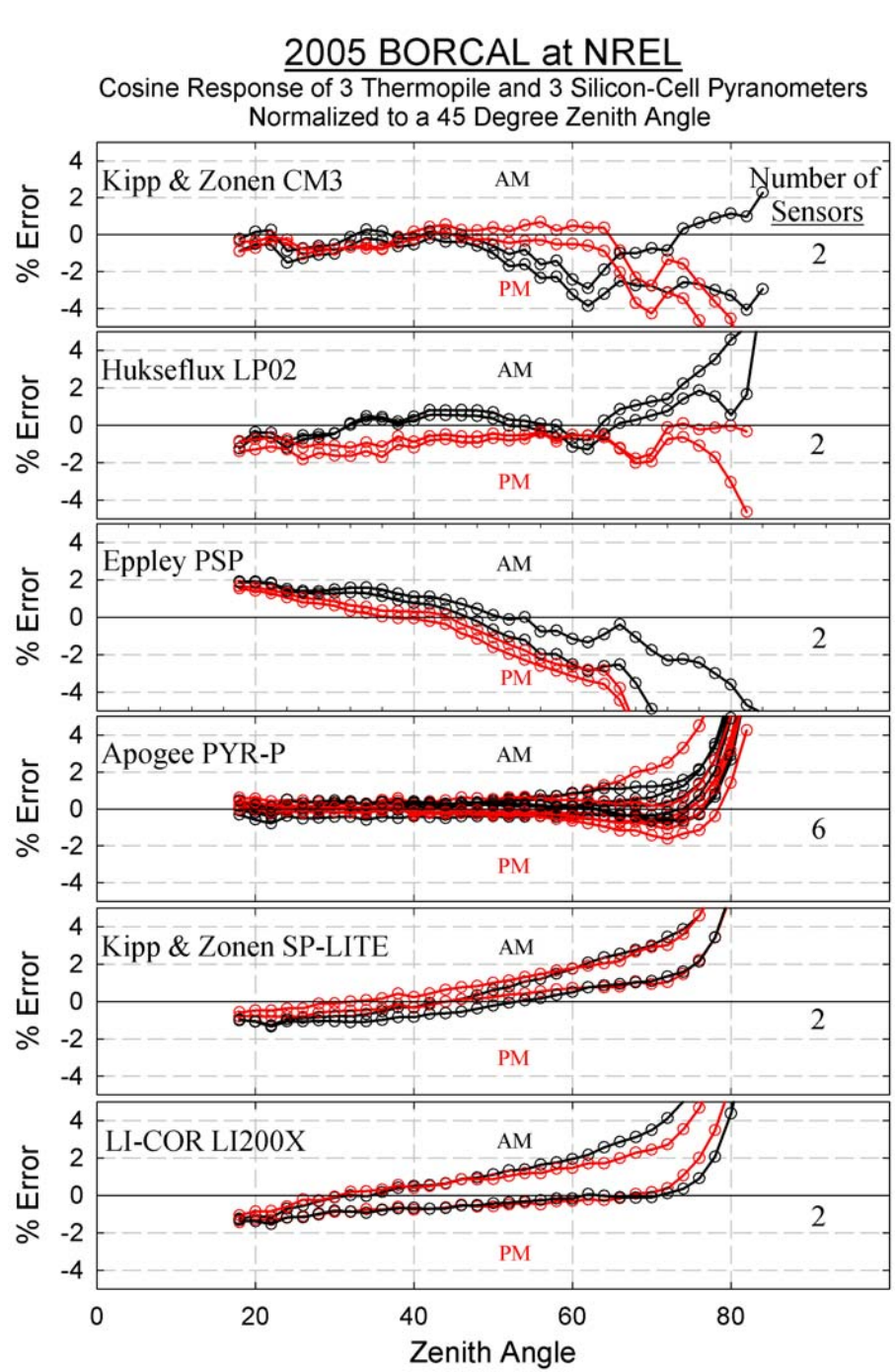
2005 BORCAL at NREL
Cosine Response of 3 Thermopile and 3 Silicon-Cell Pyranometers
Normalized to a 45 Degree Zenith Angle
Kipp & Zonen CM3
Hukseflux LP02
Eppley PSP
Apogee PYR-P
Kipp & Zonen SP-LITE
LI-COR LI200X
AM
PM
Number of Sensors
2
2
2
6
2
2
% Error
Zenith Angle

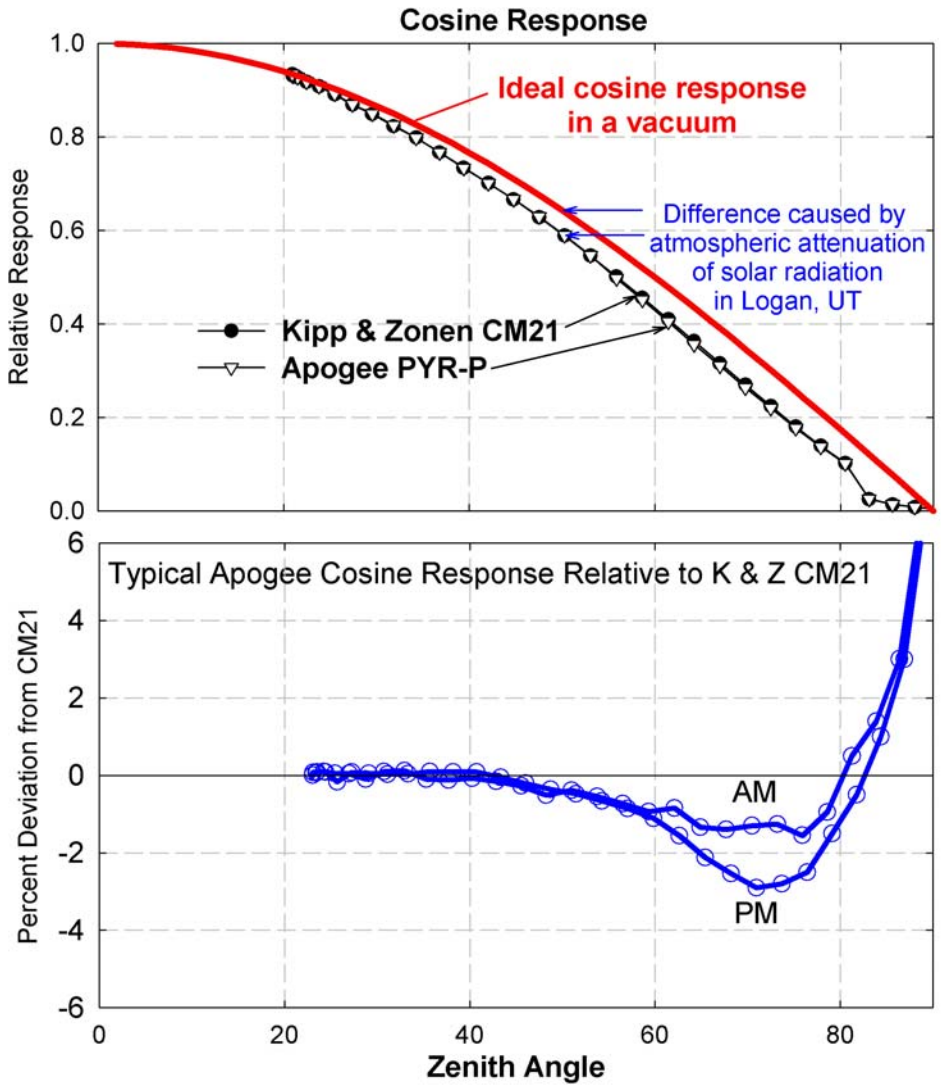
Cosine Response
Ideal cosine response in a vacuum
Difference caused by atmospheric attenuation of solar radiation in Logan, UT
Kipp & Zonen CM21
Apogee PYR-P
Relative Response
Typical Apogee Cosine Response Relative to K & Z CM21
Percent Deviation from CM21
AM
PM
Zenith Angle

Long-term Stability Oct. 2004-Oct. 2006

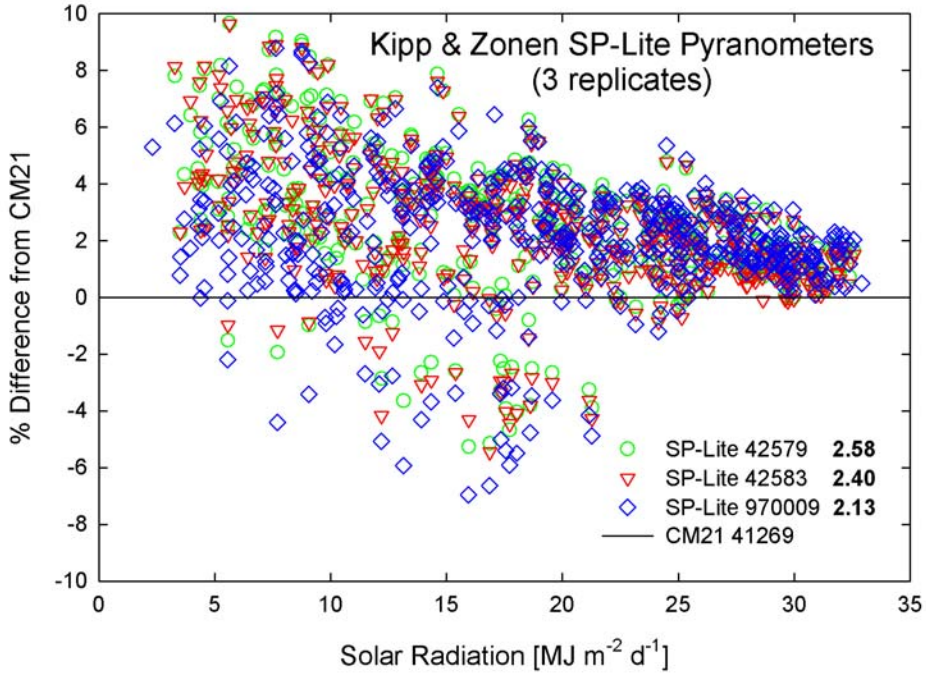

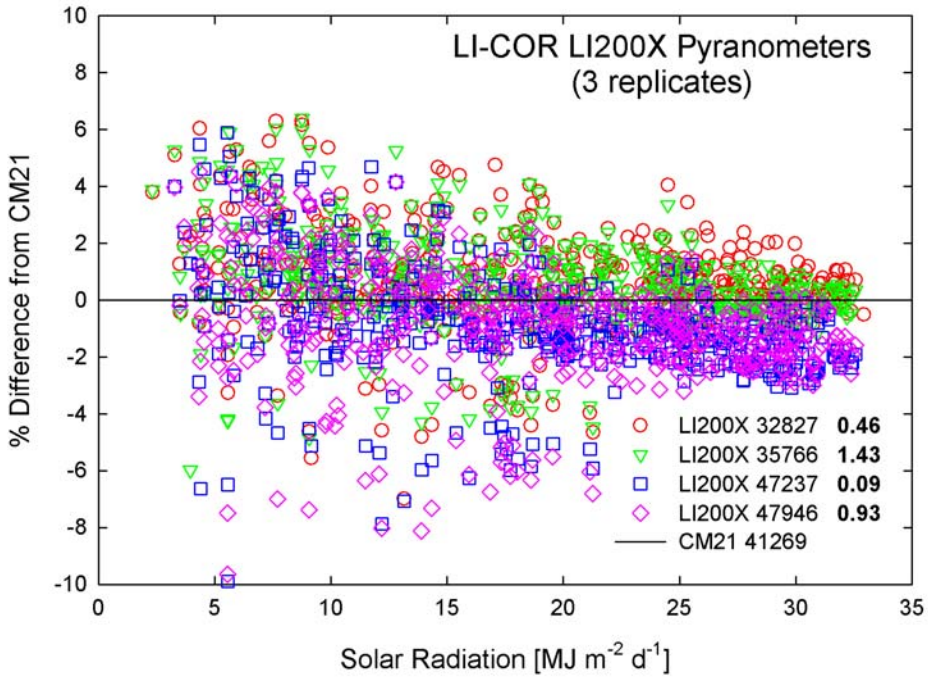

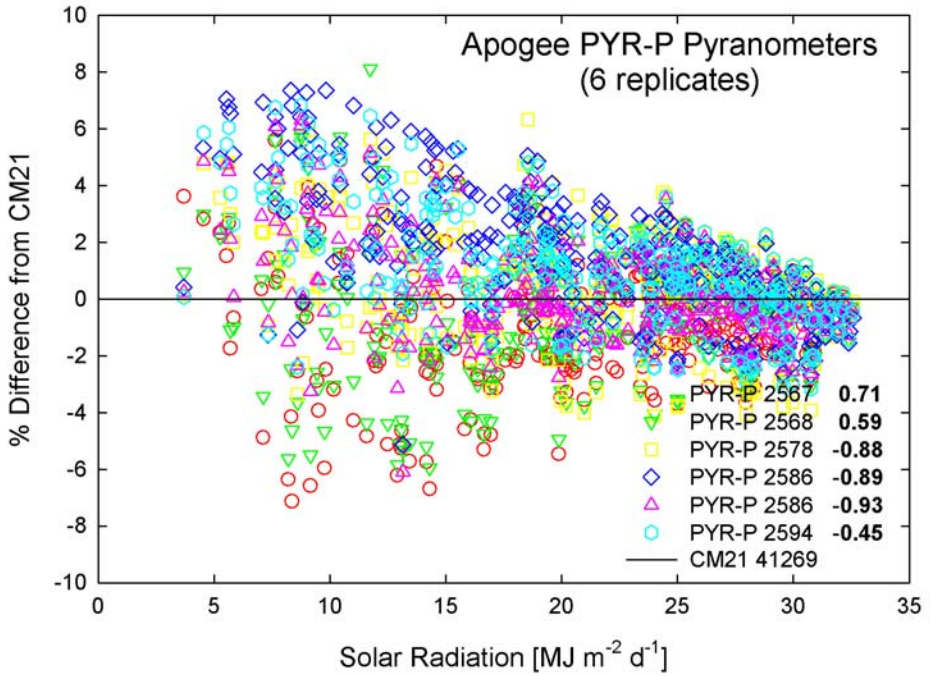

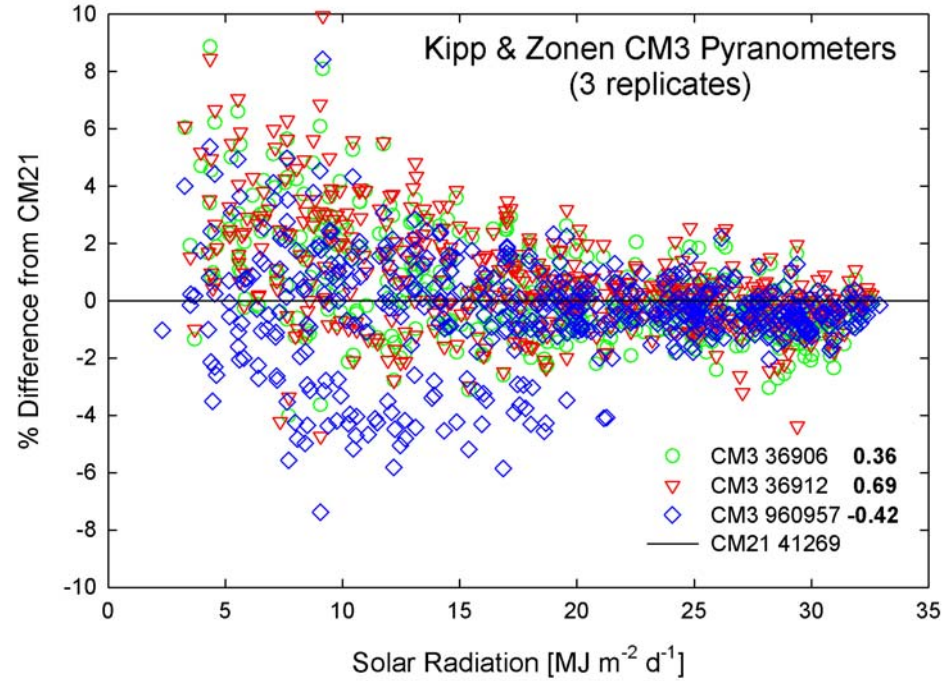
Kipp & Zonen CM3 Pyranometers
(3 replicates)
% Difference from CM21
Solar Radiation [MJ m-2 d-1]
CM3 36906 0.36
CM3 36912 0.69
CM3 960957 -0.42
CM21 41269

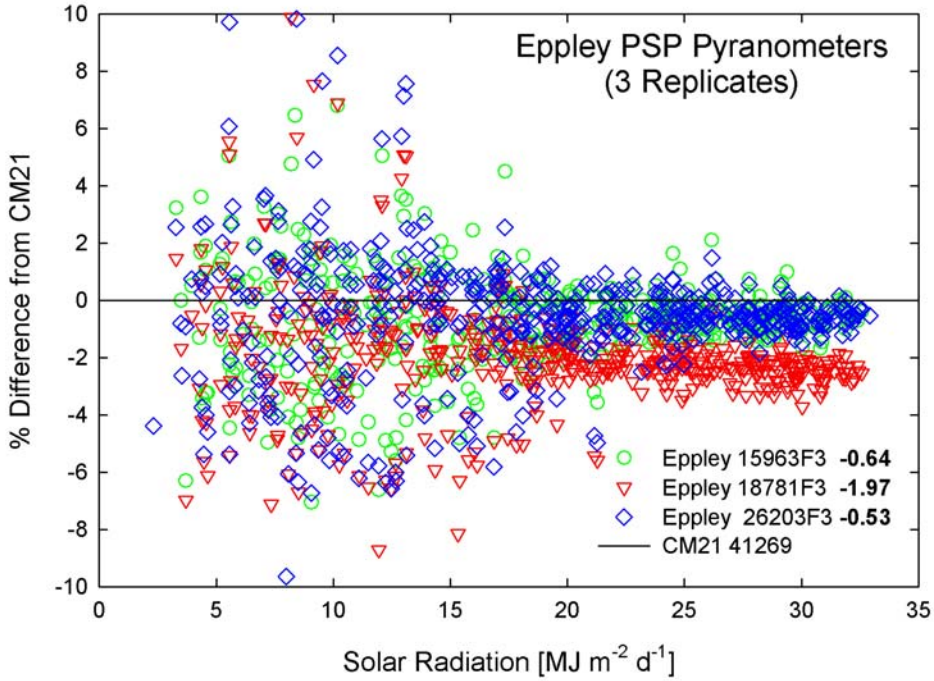
Eppley PSP Pyranometers
(3 Replicates)
% Difference from CM21
Solar Radiation [MJ m-2 d-1]
Eppley 15963F3 -0.64
Eppley 18781F3 -1.97
Eppley 26203F3 -0.53
CM21 41269

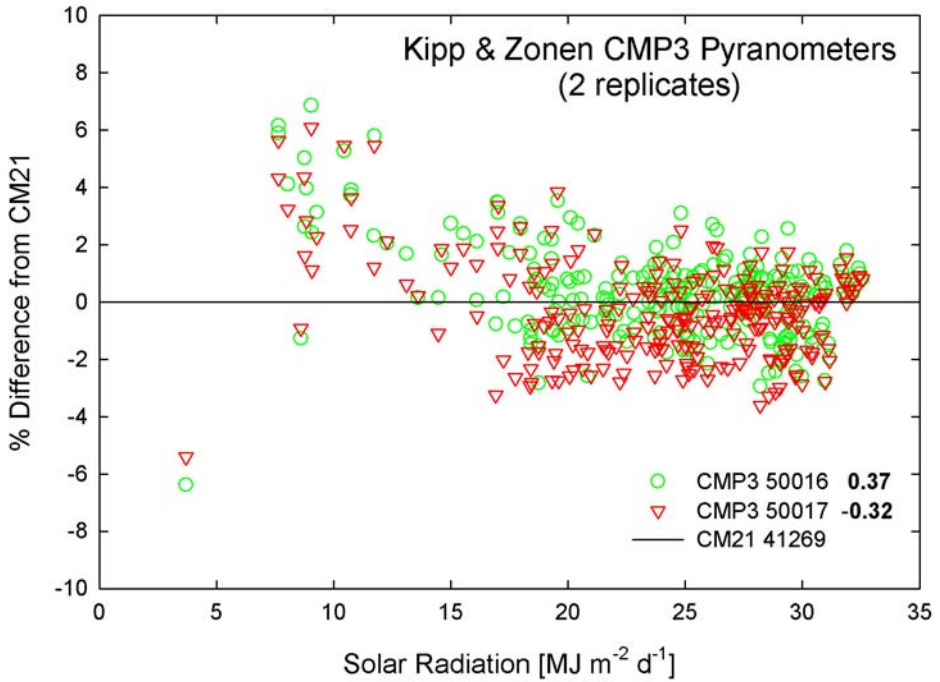
Kipp & Zonen CMP3 Pyranometers
(2 replicates)
% Difference from CM21
Solar Radiation [MJ m-2 d-1]
CMP3 50016 0.37
CMP3 50017 -0.32
CM21 41269

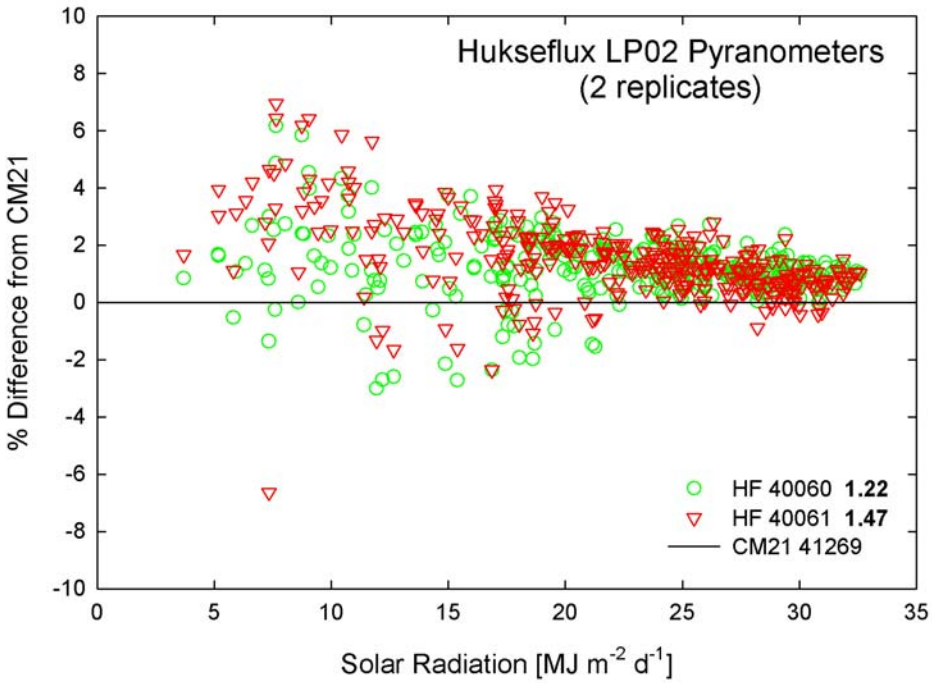
Hukseflux LP02 Pyranometers
(2 replicates)
% Difference from CM21
Solar Radiation [MJ m-2 d-1]
HF 40060 1.22
HF 40061 1.47
CM21 41269

Apogee Pyranometer Calibration

New International Headquarters for Apogee Instruments

There Goes the Neighborhood!!!